Journal of
Applied Crystallography
ISSN 0021-8898

Received 22 May 2003
Accepted 15 July 2003

© 2003 International Union of Crystallography
Printed in Great Britain – all rights reserved

The resolution function in neutron spin-echo spectroscopy with three-axis spectrometers

Klaus Habicht,[a,b]* Thomas Keller[c] and Robert Golub[a]

[a]Hahn-Meitner-Institut, Glienickerstraße 100, D-14109 Berlin, Germany, [b]Technische Universität Darmstadt, Institut für Festkörperphysik, Hochschulstraße 6, D-64289 Darmstadt, Germany, and [c]Max-Planck-Institute for Solid State Research, Heisenbergstraße 1, D-70569 Stuttgart, Germany. Correspondence e-mail: habicht@hmi.de

A resolution function for inelastic neutron spin-echo spectroscopy on a three-axis spectrometer is derived. Inelastic dispersive excitations where the tilted field technique applies are being considered. Using a Gaussian approximation of the transmission function of the three-axis spectrometer and a second-order expansion of the total Larmor phase, the instrumental resolution function of an idealized spin-echo instrument is obtained. Furthermore, the resolution function is extended to include the effects of sample properties, such as mosaicity, spread in lattice spacings and the curvature of the four-dimensional dispersion surface in a line-width measurement.

1. Introduction

Neutron spin-echo (NSE) spectroscopy increases the energy resolution accessed by conventional neutron scattering instruments by several orders of magnitude without significant loss of intensity. The method introduced by Mezei (1978) uses Larmor precession to resolve small energy changes within the resolution of a background spectrometer. In particular, the method can be applied to study lifetimes of dispersive elementary excitations in single crystals. A three-axis spectrometer (TAS) is then used as the background instrument. Precisely shaped fields tilted relative to the incident and scattered beams allow the application of the spin-echo focusing technique (Mezei, 1980; Pynn, 1978). Distinct from TAS focusing, where the resolution ellipsoid is matched to the slope of the dispersion, in spin-echo focusing the instrument parameters (tilt angles of the field boundaries and field integral ratio) are chosen so as to provide lines of constant phase which are parallel to the dispersion curve.

Since NSE spectroscopy directly measures the intermediate scattering function $I(\tau)$ the measurement sensitivity is restricted by the maximum accessible spin-echo time τ and the depolarization within this τ range. In order to extract intrinsic lifetimes from experimental data, quantitative knowledge of the instrumental resolution and other sources of signal depolarization due to sample properties, *e.g.* mosaicity, spread in lattice spacings and curvature of the dispersion surface, is of importance.

In this paper we extend the theory of inelastic neutron spin-echo spectroscopy to second order. We derive an expression for the polarization as a function of spin-echo time, assuming a dispersive excitation with zero line width of an ideal sample without lattice imperfections (§2). This is what we will call the instrumental resolution function.

The formalism is then extended to include sample imperfections. In §3 we consider the effect of mosaicity in lifetime measurements of dispersive transverse excitation modes. The modification of the resolution function due to general lattice imperfections is treated in more detail in §4. The limits of the resolution function imposed by curvature of the dispersion surface are treated in §5. Examples with typical instrumental parameters are discussed. Throughout the discussion we will use the TAS transmission function introduced by Cooper & Nathans (1967).

2. Instrumental resolution

2.1. General remarks

We consider the case of a three-axis spectrometer combined with neutron spin-echo. The NSE is idealized in the sense that stray fields or field inhomogeneities are not considered as a source of signal depolarization and the spin-echo conditions are satisfied.

Pynn (1978) has treated the TAS second-order transmission function and has combined it with the first-order approximation of the spin-echo phase, which allows one to investigate the effect of instrumental detuning. Instead, we expand the spin-echo phase up to second order and assume that spin-echo conditions are satisfied, *i.e.* the spectrometer parameters are tuned to the nominal values.

We follow the treatment of the TAS transmission function by Cooper & Nathans (1967) based on normal (Gaussian) distributions of instrumental parameters. In this framework, spatial effects such as finite dimensions of the monochromator, sample and analyser, and the monochromator or analyser focusing, are not taken into account. Real-space effects are quite accurately described by the formalism of Stoica (1975) and Popovici (1975).

The application of this formalism to the resolution function in NSE spectroscopy will be subject of future work. In the present article we will neglect finite-size effects. However, we allow the neutron beams in the first and second precession region to have finite horizontal and vertical divergence. As Dorner (1972) pointed out, the original publication of Cooper & Nathans contains a few minor errors, which are eliminated in our considerations.

The quasiparticle excitations are first assumed to follow a planar (linear) dispersion within the resolution ellipsoid of the TAS. In this case, the spin-echo fields have to be tilted. The general treatment discussed here includes dispersionless excitations as a special case.

We consider a simplified model of an NSE. We assume that neutrons are monochromated by a single-crystal monochromator. The incident neutrons with wavevector $\mathbf{k}_\mathrm{I}$ are directed along the $\mathbf{i}_1$ direction, polarized along the $\mathbf{j}_1$ direction and enter a well defined region of length L_1, containing a magnetic field B_1 pointing in the $\mathbf{l}_1$ direction (Fig. 1). The field boundaries are allowed to be tilted by an angle θ_1. The polarization is treated classically and neutrons having a polarization component perpendicular to the magnetic field will Larmor precess. After leaving the field region, the neutrons impinge on a sample where they can be scattered to a different final wavevector $\mathbf{k}_\mathrm{F}$. Some of the scattered neutrons enter a second field region of length L_2 where the field is oriented in the opposite direction to that in the first region. The field boundaries are allowed to be tilted by an angle θ_2 with respect to the scattered beam. The tilt angles are defined to be positive for anticlockwise rotation with respect to $\mathbf{k}_\mathrm{I,F}$. Scattered neutrons are analyzed in energy by a single-crystal analyser and in polarization by a polarizer. Technically these units may either be separate devices or combined (*e.g.* using Heusler analyser crystals).

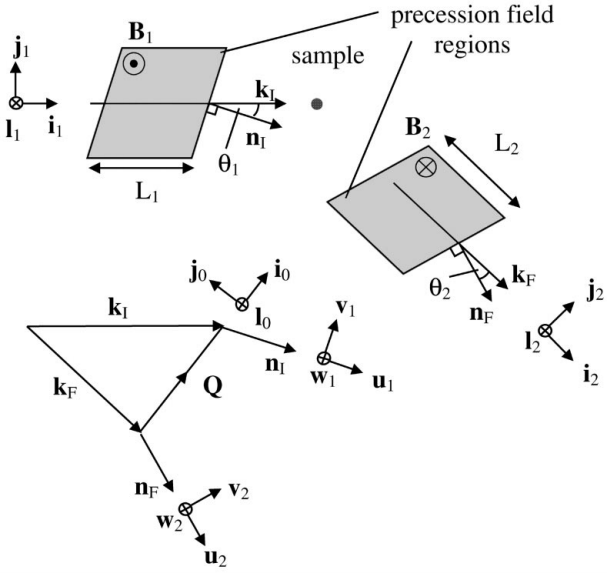

Figure 1
Schematic drawing of the precession field regions in an inelastic NSE scattering experiment.

In the general case the polarization measured by spin-echo is given by

$$P = \frac{1}{N}\int S(\mathbf{Q},\omega)T(\mathbf{k}_\mathrm{i},\mathbf{k}_\mathrm{f})\exp[i\varphi(\mathbf{k}_\mathrm{i},\mathbf{k}_\mathrm{f})]\,\mathrm{d}^3k_\mathrm{i}\,\mathrm{d}^3k_\mathrm{f} + \mathrm{c.c.} \quad (1)$$

where $S(\mathbf{Q}\,\omega)$ is the scattering function, and $T(\mathbf{k}_\mathrm{i},\mathbf{k}_\mathrm{f})$ is the TAS transmission probability. $\varphi(\mathbf{k}_\mathrm{i},\mathbf{k}_\mathrm{f})$ is the sum of Larmor precession angles before and after the sample. Here we treat φ as the classical Larmor precession angle. Alternatively, in a quantum mechanical framework, φ is a phase shift between up and down spin states, which semi-classically can be interpreted as those spin states being spatially split and delayed relative to each other (Gähler *et al.*, 1996; Keller *et al.*, 2002; Habicht *et al.*, 2003*b*). N is a normalization factor and c.c. denotes the complex conjugate of the left-hand term.

For convenience we write the total Larmor precession angle after the second field region in a vector notation:

$$\varphi = \frac{A_1}{\mathbf{k}_\mathrm{i}\cdot\mathbf{n}_\mathrm{i}} - \frac{A_2}{\mathbf{k}_\mathrm{f}\cdot\mathbf{n}_\mathrm{f}}, \quad (2)$$

where $A_{1,2} = (m/\hbar)\omega_{1,2}L_{1,2}\cos\theta_{1,2}$, with the mass of the neutron m. The wavevector $\mathbf{k}_{\mathrm{i,f}}$ denotes a general incident (scattered) wavevector and $\mathbf{n}_{\mathrm{i,f}}$ are unit vectors normal to the field boundaries of the precession regions before and after the sample. The Larmor frequency is given by

$$\omega_{1,2} = \gamma B_{1,2}, \quad (3)$$

where the gyromagnetic ratio of the neutron $\gamma = 2\pi \times 2.916$ kHz G^{-1}. In the special case of neutron resonance spin-echo (NRSE), $A_{1,2} = (2\pi m\hbar)\nu_{1,2}^{\mathrm{eff}}L_{1,2}\cos\theta_{1,2}$. Here $\nu_{1,2}^{\mathrm{eff}}$ refers to the effective frequency, which is the frequency applied to the RF flippers times a factor of 2 or 4 depending on the number of RF flippers operated. The distances $L_{1,2}$ refer to the coil separation in the first and second spin-echo arm, respectively. See *e.g.* Keller *et al.* (2002) for details of the resonance spin-echo technique.

2.2. First-order expansion of the spin-echo phase and spin-echo conditions

The derivation of the spin-echo conditions for inelastic, dispersive excitations can be found elsewhere (Keller *et al.*, 2002; Habicht *et al.*, 2003*b*). Here we give a short review for continuity of notation and later reference.

The point of spin-echo focusing is that the total Larmor precession angle expanded to first order will not depend on small variations in momentum variables for a special choice of instrumental parameters but, apart from a constant φ_0, only depends on energy deviations from the (planar) dispersion surface, *i.e.*

$$\varphi - \varphi_0 = -\tau\Delta\omega, \quad (4)$$

where $\Delta\omega = \omega(\mathbf{q}) - \omega_0(\mathbf{q})$. Here $\mathbf{q}$ is the wavevector of the quasiparticle and $\omega_0(\mathbf{q})$ denotes the nominal energy of the excitation if there were no line broadening. τ is the spin-echo time. This definition of $\Delta\omega$ is different from the usual TAS language, where energy deviations are always given relative to

$\omega_0(\mathbf{q}_0)$, the centre of the resolution ellipsoid for a given setting of the TAS.

Expanding the total Larmor precession angle to first order for the general case of tilted field boundaries relative to the incident and scattered beams, we have

$$\varphi - \varphi_0 = -\frac{A_1}{(\mathbf{k}_\mathrm{I}\cdot\mathbf{n}_\mathrm{i})^2}(\Delta\mathbf{k}_\mathrm{i}\cdot\mathbf{n}_\mathrm{i}) + \frac{A_2}{(\mathbf{k}_\mathrm{F}\cdot\mathbf{n}_\mathrm{f})^2}(\Delta\mathbf{k}_\mathrm{f}\cdot\mathbf{n}_\mathrm{f}), \quad (5)$$

where $\mathbf{k}_\mathrm{I}$, $\mathbf{k}_\mathrm{F}$ refer to the central values of incident and final wavevectors and $\Delta\mathbf{k}_\mathrm{i}$, $\Delta\mathbf{k}_\mathrm{f}$ to the corresponding variations, *i.e.* $\mathbf{k}_{\mathrm{i,f}} = \mathbf{k}_{\mathrm{I,F}} + \Delta\mathbf{k}_{\mathrm{i,f}}$.

We use energy and momentum conservation to change variables and express $\Delta\omega$ as a function of $\Delta\mathbf{k}_\mathrm{i}$ and $\Delta\mathbf{k}_\mathrm{f}$. To first order

$$\hbar\omega(\mathbf{q}) = \frac{\hbar^2}{2m}\left[\mathbf{k}_\mathrm{I}^2 - \mathbf{k}_\mathrm{F}^2 + 2(\mathbf{k}_\mathrm{I}\cdot\Delta\mathbf{k}_\mathrm{i}) - 2(\mathbf{k}_\mathrm{F}\cdot\Delta\mathbf{k}_\mathrm{f})\right]. \quad (6)$$

Since

$$\hbar\omega_0(\mathbf{q}_0) = \frac{\hbar^2}{2m}(\mathbf{k}_\mathrm{I}^2 - \mathbf{k}_\mathrm{F}^2), \quad (7)$$

we can write

$$\omega(\mathbf{q}) - \omega_0(\mathbf{q}_0) = \frac{\hbar}{m}\left[(\mathbf{k}_\mathrm{I}\cdot\Delta\mathbf{k}_\mathrm{i}) - (\mathbf{k}_\mathrm{F}\cdot\Delta\mathbf{k}_\mathrm{f})\right]. \quad (8)$$

We assume a planar dispersion relation, a restriction later to be relaxed, and can expand the dispersion relation to first order in $(\mathbf{q}-\mathbf{q}_0)$ such that we have

$$\omega(\mathbf{q}) - \omega_0(\mathbf{q}_0) = \Delta\omega + \nabla_q\omega_0(\mathbf{q}_0)\cdot(\mathbf{q}-\mathbf{q}_0). \quad (9)$$

Combining (8) and (9) yields

$$\Delta\omega = \frac{\hbar}{m}\left[(\mathbf{k}_\mathrm{I}\cdot\Delta\mathbf{k}_\mathrm{i}) - (\mathbf{k}_\mathrm{F}\cdot\Delta\mathbf{k}_\mathrm{f})\right] - \nabla_q\omega_0(\mathbf{q}_0)\cdot(\mathbf{q}-\mathbf{q}_0). \quad (10)$$

Since the momentum of the excitation in a perfect crystal is

$$\mathbf{q}_0 = \mathbf{k}_\mathrm{I} - \mathbf{k}_\mathrm{F} - \mathbf{G}_0, \quad (11)$$

$$\mathbf{q} = \mathbf{k}_\mathrm{i} - \mathbf{k}_\mathrm{f} - \mathbf{G}_0, \quad (12)$$

($\mathbf{G}_0$ is a reciprocal-lattice vector) we have

$$\mathbf{q} - \mathbf{q}_0 = \Delta\mathbf{k}_\mathrm{i} - \Delta\mathbf{k}_\mathrm{f}. \quad (13)$$

The restriction to a perfect crystal will be relaxed later. Now we have

$$-\tau\Delta\omega = -\tau\left[\frac{\hbar}{m}\mathbf{k}_\mathrm{I} - \nabla_q\omega_0(\mathbf{q}_0)\right]\cdot\Delta\mathbf{k}_\mathrm{i} + \tau\left[\frac{\hbar}{m}\mathbf{k}_\mathrm{F} - \nabla_q\omega_0(\mathbf{q}_0)\right]\cdot\Delta\mathbf{k}_\mathrm{f}. \quad (14)$$

Comparing the coefficients of $\Delta\mathbf{k}_\mathrm{i}$, $\Delta\mathbf{k}_\mathrm{f}$ in (5) and (14) we obtain the normal vectors to the field boundaries,

$$\mathbf{n}_{\mathrm{i,f}} = \frac{(\hbar/m)\mathbf{k}_{\mathrm{I,F}} - \nabla_q\omega_0(\mathbf{q}_0)}{|(\hbar/m)\mathbf{k}_{\mathrm{I,F}} - \nabla_q\omega_0(\mathbf{q}_0)|}, \quad (15)$$

and identify the spin-echo time τ with

$$\tau = \frac{A_{1,2}}{(\mathbf{k}_{\mathrm{I,F}}\cdot\mathbf{n}_\mathrm{i})^2|(\hbar/m)\mathbf{k}_{\mathrm{I,F}} - \nabla_q\omega_0(\mathbf{q}_0)|}. \quad (16)$$

For equal coil distances in the first and second arm, the frequency ratio is then given by

$$\frac{\nu_1}{\nu_2} = \frac{\cos\theta_2}{\cos\theta_1}\frac{(\mathbf{k}_\mathrm{I}\cdot\mathbf{n}_\mathrm{i})^2|(\hbar/m)\mathbf{k}_\mathrm{I} - \nabla_q\omega_0(\mathbf{q}_0)|}{(\mathbf{k}_\mathrm{F}\cdot\mathbf{n}_\mathrm{f})^2|(\hbar/m)\mathbf{k}_\mathrm{F} - \nabla_q\omega_0(\mathbf{q}_0)|}. \quad (17)$$

The basic idea of spin-echo focusing is to remove any momentum dependence of the total Larmor angle even in the presence of finite dispersion. With NRSE this is achieved by choosing the tilt angles of the RF coils θ_1, θ_2 and the frequency ratio ν_1/ν_2 to satisfy the spin-echo conditions (15) and (17). The spin-echo time is given by equation (16). In a more rigorous treatment (Keller *et al.*, 2002) it has been shown that τ can be interpreted as a relative delay of up and down wavepackets and it becomes apparent that τ is identical to the correlation time, which is the fundamental variable in the time-dependent van Hove density–density correlation function.

We note that the independence of the Larmor phase φ of any of the total momentum transfer variables $\hbar\mathbf{Q}$ is strictly true only for a first-order approximation of the total Larmor phase and a perfect match of the spin-echo conditions.

We consider the scattering function $S(\mathbf{Q},\omega)$ of a dispersive excitation and assume the line width and S($\mathbf{Q}$) to be independent of $\mathbf{Q}$ in that part of the dispersion surface which is located within the TAS resolution ellipsoid. Hence we can integrate over the momentum components and therefore

$$P \propto \int S(\Delta\omega)T(\Delta\omega)\exp(i\varphi)\,\mathrm{d}\Delta\omega + \text{c.c.} \quad (18)$$

with $\Delta\omega$ given by equation (10). As opposed to conventional TAS spectroscopy, neutron spin-echo spectroscopy will only be applied if the width of the excitation $S(\Delta\omega)$ is much less than the TAS energy resolution $T(\Delta\omega)$. In this case $T(\Delta\omega)$ can be considered to be constant. Hence the polarization directly yields the cosine Fourier transform of the line shape:

$$P \propto \int S(\Delta\omega)\cos(\tau\Delta\omega)\,\mathrm{d}\Delta\omega. \quad (19)$$

It should be noted that the phase φ_0 causes a rapid oscillation of the spin-echo signal with substantial importance for the experiment. Here, however, we are only interested in the 'envelope' of this rapidly oscillating function, which is independent of φ_0.

For a Lorentzian line shape, the polarization follows a simple exponential decay:

$$P(\tau) = \exp(-\Gamma\tau), \quad (20)$$

where Γ is the HWHM (half width at half-maximum) line width.

2.3. Second-order expansion of the spin-echo phase

We will now discuss the Larmor phase in a second-order approximation to include resolution effects. Expanding equation (2) to second order we have

$$\varphi = \varphi_0 - \frac{A_1}{(\mathbf{k}_\mathrm{I}\cdot\mathbf{n}_\mathrm{i})^2}(\Delta\mathbf{k}_\mathrm{i}\cdot\mathbf{n}_\mathrm{i}) + \frac{A_2}{(\mathbf{k}_\mathrm{F}\cdot\mathbf{n}_\mathrm{f})^2}(\Delta\mathbf{k}_\mathrm{f}\cdot\mathbf{n}_\mathrm{f}) + \frac{A_1}{(\mathbf{k}_\mathrm{I}\cdot\mathbf{n}_\mathrm{i})^3}(\Delta\mathbf{k}_\mathrm{i}\cdot\mathbf{n}_\mathrm{i})^2 - \frac{A_2}{(\mathbf{k}_\mathrm{F}\cdot\mathbf{n}_\mathrm{f})^3}(\Delta\mathbf{k}_\mathrm{f}\cdot\mathbf{n}_\mathrm{f})^2. \quad (21)$$

Here $\mathbf{k}_{\mathrm{I,F}}$ are the most probable wavevectors. φ is only a function of the scalar wavenumber variables x_1, y_1, x_2, y_2 if we use the definitions

$$\Delta\mathbf{k}_\mathrm{i} = x_1\mathbf{i}_1 + y_1\mathbf{j}_1 + z_1\mathbf{l}_1 \quad (22)$$

and

$$\Delta\mathbf{k}_\mathrm{f} = x_2\mathbf{i}_2 + y_2\mathbf{j}_2 + z_2\mathbf{l}_2 \quad (23)$$

and assume tilted fields such that

$$\mathbf{n}_\mathrm{i} = \cos\theta_1\mathbf{i}_1 + \sin\theta_1\mathbf{j}_1 \quad (24)$$

and

$$\mathbf{n}_\mathrm{f} = \cos\theta_2\mathbf{i}_2 + \sin\theta_2\mathbf{j}_2. \quad (25)$$

See Fig. 1 for the definition of the vectors **i**, **j**, **k** and **n**. Since the precession angle can only depend on wavevector components perpendicular to the field boundaries, there is no dependence on wavevector components z_1, z_2 perpendicular to the scattering plane.

Writing the energy conservation in second order we have

$$\Delta\omega = N_\mathrm{I}\mathbf{n}_\mathrm{i}\cdot\Delta\mathbf{k}_\mathrm{i} - N_\mathrm{F}\mathbf{n}_\mathrm{f}\cdot\Delta\mathbf{k}_\mathrm{f} + \frac{\hbar}{2m}(\Delta\mathbf{k}_\mathrm{i}^2 - \Delta\mathbf{k}_\mathrm{f}^2), \quad (26)$$

where the first two terms on the right side follow directly from equations (14) and (15) and we have defined

$$N_{\mathrm{I,F}} = \left|\frac{\hbar}{m}\mathbf{k}_{\mathrm{I,F}} - \nabla_q\omega_0(\mathbf{q}_0)\right|. \quad (27)$$

Rewriting equation (26) we can express $\Delta\mathbf{k}_\mathrm{f}\cdot\mathbf{n}_\mathrm{f}$ in terms of $\Delta\omega$, $\mathbf{n}_\mathrm{i}\cdot\Delta\mathbf{k}_\mathrm{i}$ and $\Delta\mathbf{k}_\mathrm{f}^2$, *i.e.*

$$\Delta\mathbf{k}_\mathrm{f}\cdot\mathbf{n}_\mathrm{f} = \frac{1}{N_\mathrm{F}}\left[-\Delta\omega + N_\mathrm{I}\mathbf{n}_\mathrm{i}\cdot\Delta\mathbf{k}_\mathrm{i} + \frac{\hbar}{2m}(\Delta\mathbf{k}_\mathrm{i}^2 - \Delta\mathbf{k}_\mathrm{f}^2)\right]. \quad (28)$$

We now substitute $(\Delta\mathbf{k}_\mathrm{f}\cdot\mathbf{n}_\mathrm{f})$ in equation (21) with the result

$$\varphi - \varphi_0 = -\frac{A_2}{(\mathbf{k}_\mathrm{F}\cdot\mathbf{n}_\mathrm{f})^2}\frac{1}{N_\mathrm{F}}\Delta\omega + \left[-\frac{A_1}{(\mathbf{k}_\mathrm{I}\cdot\mathbf{n}_\mathrm{i})^2} + \frac{A_2}{(\mathbf{k}_\mathrm{F}\cdot\mathbf{n}_\mathrm{f})^2}\frac{N_\mathrm{I}}{N_\mathrm{F}}\right](\mathbf{n}_\mathrm{i}\cdot\Delta\mathbf{k}_\mathrm{i}) + \frac{\hbar}{2m}\frac{A_2}{(\mathbf{k}_\mathrm{F}\cdot\mathbf{n}_\mathrm{f})^2}\frac{1}{N_\mathrm{F}}[(\Delta\mathbf{k}_\mathrm{i}^2 - \Delta\mathbf{k}_\mathrm{f}^2)] + \frac{A_1}{(\mathbf{k}_\mathrm{I}\cdot\mathbf{n}_\mathrm{i})^3}(\Delta\mathbf{k}_\mathrm{i}\cdot\mathbf{n}_\mathrm{i})^2 - \frac{A_2}{(\mathbf{k}_\mathrm{F}\cdot\mathbf{n}_\mathrm{f})^3}\left\{\frac{1}{N_\mathrm{F}}\left[-\Delta\omega + N_\mathrm{I}\mathbf{n}_\mathrm{i}\cdot\Delta\mathbf{k}_\mathrm{i} + \frac{\hbar}{2m}(\Delta\mathbf{k}_\mathrm{i}^2 - \Delta\mathbf{k}_\mathrm{f}^2)\right]\right\}^2. \quad (29)$$

We assume that the spin-echo parameters are set such that the spin-echo conditions (15) and (17) are satisfied, *i.e.* the expression in the first set of square brackets will vanish, and introduce τ as defined in equation (16). Neglecting the terms higher than second order,

$$\varphi - \varphi_0 = -\tau\Delta\omega + \tau\left[\frac{\hbar}{2m}(\Delta\mathbf{k}_\mathrm{i}^2 - \Delta\mathbf{k}_\mathrm{f}^2)\right] + \tau\frac{N_\mathrm{I}}{(\mathbf{k}_\mathrm{I}\cdot\mathbf{n}_\mathrm{i})}(\Delta\mathbf{k}_\mathrm{i}\cdot\mathbf{n}_\mathrm{i})^2 - \tau\frac{1}{N_\mathrm{F}(\mathbf{k}_\mathrm{F}\cdot\mathbf{n}_\mathrm{f})}[-\Delta\omega + N_\mathrm{I}(\Delta\mathbf{k}_\mathrm{i}\cdot\mathbf{n}_\mathrm{i})]^2. \quad (30)$$

The elimination of the $\Delta\mathbf{k}_\mathrm{f}^2$ term remains. In equation (23), $\Delta\mathbf{k}_\mathrm{f}$ is written in Cartesian coordinates with $\mathbf{i}_2$ pointing along $\mathbf{k}_\mathrm{F}$. However, it is more convenient to transform $\Delta\mathbf{k}_\mathrm{f}$ (and $\Delta\mathbf{k}_\mathrm{i}$) to coordinates with $\mathbf{u}_2$ ($\mathbf{u}_1$) pointing along $\mathbf{n}_\mathrm{f}$ ($\mathbf{n}_\mathrm{i}$) (see Fig. 1 for a definition of these vectors); then

$$\Delta\mathbf{k}_\mathrm{f} = (\Delta\mathbf{k}_\mathrm{f}\cdot\mathbf{n}_\mathrm{f})\mathbf{u}_2 + \left[-\tan\theta_2(\Delta\mathbf{k}_\mathrm{f}\cdot\mathbf{n}_\mathrm{f}) + y_2\frac{1}{\cos\theta_2}\right]\mathbf{v}_2 + z_2\mathbf{w}_2 \quad (31)$$

and

$$\Delta\mathbf{k}_\mathrm{i} = (\Delta\mathbf{k}_\mathrm{i}\cdot\mathbf{n}_\mathrm{i})\mathbf{u}_1 + \left[-\tan\theta_1(\Delta\mathbf{k}_\mathrm{i}\cdot\mathbf{n}_\mathrm{i}) + y_1\frac{1}{\cos\theta_1}\right]\mathbf{v}_1 + z_1\mathbf{w}_1. \quad (32)$$

It is sufficient to use equation (28) to first order for substitution of $\Delta\mathbf{k}_\mathrm{f}\cdot\mathbf{n}_\mathrm{f}$ in equation (31) so that

$$\Delta\mathbf{k}_\mathrm{f}^2 = \left[\frac{1}{N_\mathrm{F}}(-\Delta\omega + N_\mathrm{I}\mathbf{n}_\mathrm{i}\cdot\Delta\mathbf{k}_\mathrm{i})\right]^2 + \left\{-\tan\theta_2\left[\frac{1}{N_\mathrm{F}}(-\Delta\omega + N_\mathrm{I}\mathbf{n}_\mathrm{i}\cdot\Delta\mathbf{k}_\mathrm{i})\right] + y_2\frac{1}{\cos\theta_2}\right\}^2 + z_2^2. \quad (33)$$

We have also

$$\Delta\mathbf{k}_\mathrm{i}^2 = \Delta k_\mathrm{in}^2 + \left(-\Delta k_\mathrm{in}\tan\theta_1 + y_1\frac{1}{\cos\theta_1}\right)^2 + z_1^2 \quad (34)$$

with

$$\Delta k_\mathrm{in} = \Delta\mathbf{k}_\mathrm{i}\cdot\mathbf{n}_\mathrm{i}. \quad (35)$$

Substituting equations (33) and (34) into equation (29) and combining squared and cross terms of $\Delta\omega$, Δk_in, y_1, y_2, z_1, z_2, the expression for the total Larmor precession angle in second order is now

$$\begin{aligned}\varphi - \varphi_0 = {} & -\tau\Delta\omega - \tfrac{1}{2}\tau\Psi_{55}z_1^2 - \tfrac{1}{2}\tau\Psi_{66}z_2^2 - \tfrac{1}{2}\tau\Psi_{11}\Delta\omega^2 \\ & - \tfrac{1}{2}\tau\Psi_{22}\Delta k_\mathrm{in}^2 - \tau\Psi_{12}\Delta\omega\Delta k_\mathrm{in} - \tfrac{1}{2}\tau\Psi_{33}y_1^2 \\ & - \tau\Psi_{23}\Delta k_\mathrm{in}y_1 - \tfrac{1}{2}\tau\Psi_{44}y_2^2 - \tau\Psi_{24}\Delta k_\mathrm{in}y_2 \\ & - \tau\Psi_{14}\Delta\omega y_2, \end{aligned} \quad (36)$$

where we have defined

$$\Psi_{11} = \frac{\hbar}{m}\frac{1}{N_\mathrm{F}^2\cos^2\theta_2} + \frac{2}{N_\mathrm{F}(\mathbf{k}_\mathrm{F}\cdot\mathbf{n}_\mathrm{f})}, \quad (37)$$

$$\Psi_{22} = -\frac{\hbar}{m}\frac{1}{\cos^2\theta_1} + \frac{\hbar}{m}\frac{N_\mathrm{I}^2}{N_\mathrm{F}^2}\frac{1}{\cos^2\theta_2} - \frac{2N_\mathrm{I}}{(\mathbf{k}_\mathrm{I}\cdot\mathbf{n}_\mathrm{i})} + \frac{2N_\mathrm{I}^2}{N_\mathrm{F}(\mathbf{k}_\mathrm{F}\cdot\mathbf{n}_\mathrm{f})}, \quad (38)$$

$$\Psi_{33} = -\frac{\hbar}{m}\frac{1}{\cos^2\theta_1}, \quad \Psi_{44} = \frac{\hbar}{m}\frac{1}{\cos^2\theta_2}, \quad (39)$$

$$\Psi_{55} = -\frac{\hbar}{m}, \quad \Psi_{66} = +\frac{\hbar}{m}, \tag{40}$$

$$\Psi_{12} = -\frac{\hbar}{m}\frac{N_\mathrm{I}}{N_\mathrm{F}^2}\frac{1}{\cos^2\theta_2} - \frac{2N_\mathrm{I}}{N_\mathrm{F}(\mathbf{k}_\mathrm{F}\cdot\mathbf{n}_\mathrm{f})}, \tag{41}$$

$$\Psi_{14} = \frac{\hbar}{m}\frac{\tan\theta_2}{\cos\theta_2}\frac{1}{N_\mathrm{F}}, \tag{42}$$

$$\Psi_{23} = \frac{\hbar}{m}\frac{\tan\theta_1}{\cos\theta_1}, \tag{43}$$

$$\Psi_{24} = -\frac{\hbar}{m}\frac{\tan\theta_2}{\cos\theta_2}\frac{N_\mathrm{I}}{N_\mathrm{F}}. \tag{44}$$

As we will see later, it is advantageous to express the Larmor phase expanded to second order in a matrix notation. The matrix approach to the resolution problem in neutron instrumentation has been introduced by Stoica (1975) and applied to the TAS resolution problem by Popovici (1975).

We define the six-component column vector $\mathbf{J} = (\Delta\omega, \Delta k_\mathrm{in}, y_1, y_2, z_1, z_2)$ and the symmetric (6×6) matrix $\mathbf{\Psi}$. $\mathbf{\Psi}$ has non-zero elements as given above.

Finally, we can write the total Larmor phase in the compact form

$$\exp[i(\varphi - \varphi_0)] = \exp(-i\tau\Delta\omega)\exp\left(-\tfrac{1}{2}i\tau\mathbf{J}^T\mathbf{\Psi}\mathbf{J}\right). \tag{45}$$

Summarizing, we have expanded the total Larmor precession angle φ to second order. We have assumed that the spin-echo conditions (15) and (17) are satisfied. Using a transform of variables, φ is formulated as a function of the variables $\Delta\omega$, Δk_in, y_1, y_2, z_1, z_2. The only linear dependence is in $\Delta\omega$. All other terms are of second order and are proportional to the spin-echo time τ. A more compact formulation of the second-order Larmor phase is obtained in a matrix notation, which we will make use of when performing the necessary integrations in equation (1).

2.4. Three-axis transmission function

We now treat the transmission probability through the three-axis instrument. We start from the expression derived by Cooper & Nathans (1967):

$$\begin{aligned} T(\mathbf{k}_\mathrm{i}, \mathbf{k}_\mathrm{f}) &= \exp(\Omega) \\ &= \exp\Big[-\tfrac{1}{2}\big(b_5x_1^2 + 2b_0x_1y_1 + b_1y_1^2 + b_3x_2^2 \\ &\quad + 2b_4x_2y_2 + b_2y_2^2 + a_{11}^2z_1^2 + a_{12}^2z_2^2\big)\Big]. \end{aligned} \tag{46}$$

The quantities b_{0-5} and a_{11}^2, a_{12}^2 are defined in Appendix *A*. Writing $\Delta\mathbf{k}_\mathrm{i}$ and $\Delta\mathbf{k}_\mathrm{f}$ in the $(\mathbf{u}_{1,2}, \mathbf{v}_{1,2}, \mathbf{w}_{1,2})$ coordinate system and using equation (28) up to first order, we transform the variables

$$x_1 = \frac{1}{\cos\theta_1}\Delta k_\mathrm{in} - y_1\tan\theta_1 \tag{47}$$

and

$$x_2 = \frac{1}{\cos\theta_2}\left(\frac{N_\mathrm{I}}{N_\mathrm{F}}\Delta k_\mathrm{in} - \frac{1}{N_\mathrm{F}}\Delta\omega\right) - y_2\tan\theta_2. \tag{48}$$

Using the same combination of squared and cross terms of $\Delta\omega$, Δk_in, y_1, y_2, z_1, z_2 as before for the Larmor phase, the exponent Ω can be expressed as

$$\begin{aligned} \Omega = &-\tfrac{1}{2}\Xi_{11}\Delta\omega^2 - \tfrac{1}{2}\Xi_{22}\Delta k_\mathrm{in}^2 - \Xi_{12}\Delta k_\mathrm{in}\Delta\omega - \tfrac{1}{2}\Xi_{33}y_1^2 \\ &- \Xi_{23}\Delta k_\mathrm{in}y_1 - \tfrac{1}{2}\Xi_{44}y_2^2 - \Xi_{24}\Delta k_\mathrm{in}y_2 - \Xi_{14}\Delta\omega y_2 \\ &- \tfrac{1}{2}\Xi_{55}z_1^2 - \tfrac{1}{2}\Xi_{66}z_2^2, \end{aligned} \tag{49}$$

with the definitions

$$\Xi_{11} = \frac{b_3}{\cos^2\theta_2}\frac{1}{N_\mathrm{F}^2}, \tag{50}$$

$$\Xi_{22} = \frac{b_5}{\cos^2\theta_1} + \frac{b_3}{\cos^2\theta_2}\frac{N_\mathrm{I}^2}{N_\mathrm{F}^2}, \tag{51}$$

$$\Xi_{33} = b_5\tan^2\theta_1 + b_1 - b_0\tan\theta_1, \tag{52}$$

$$\Xi_{44} = -2b_4\tan\theta_2 + b_2 + b_3\tan^2\theta_2 \tag{53}$$

$$\Xi_{55} = a_{11}^2, \quad \Xi_{66} = a_{12}^2, \tag{54}$$

$$\Xi_{12} = -\frac{b_3}{\cos^2\theta_2}\frac{N_\mathrm{I}}{N_\mathrm{F}^2}, \tag{55}$$

$$\Xi_{14} = \frac{b_3\tan\theta_2}{\cos\theta_2}\frac{1}{N_\mathrm{F}} - \frac{b_4}{\cos\theta_2}\frac{1}{N_\mathrm{F}}, \tag{56}$$

$$\Xi_{23} = -\frac{b_5}{\cos\theta_1}\tan\theta_1 + \frac{b_0}{\cos\theta_1}, \tag{57}$$

$$\Xi_{24} = \frac{b_3\tan\theta_2}{\cos\theta_2}\frac{N_\mathrm{I}}{N_\mathrm{F}} + \frac{b_4}{\cos\theta_2}\frac{N_\mathrm{I}}{N_\mathrm{F}}. \tag{58}$$

Analogous to the Larmor phase expanded to second order, we will also express the Cooper–Nathans exponent Ω in a matrix notation using the column vector $\mathbf{J} = \Delta\omega$, Δk_in, y_1, y_2, z_1, z_2 and the symmetric (6×6) matrix $\mathbf{\Xi}$. The matrix $\mathbf{\Xi}$ has non-zero elements as defined above. We can therefore write the TAS transmission probability

$$\exp(\Omega) = \exp(-\tfrac{1}{2}\mathbf{J}^T\mathbf{\Xi}\mathbf{J}). \tag{59}$$

2.5. The τ dependence of the polarization

We can now reformulate equation (1) to read

$$P = \frac{1}{N}\int S(\mathbf{Q},\omega)\exp(-i\tau\Delta\omega)\exp\left(-\tfrac{1}{2}\mathbf{J}^T\mathbf{L}_\mathrm{I}\mathbf{J}\right)\mathrm{d}J_n + \text{c.c.} \tag{60}$$

where we have defined

$$\mathbf{L}_\mathrm{I}(\tau) = \mathbf{\Xi} + i\tau\mathbf{\Psi}. \tag{61}$$

We assume again that $S(\mathbf{Q},\omega)$ = constant $\times$ $S(\Delta\omega)$. Furthermore, we can neglect the terms quadratic in $\Delta\omega$ and cross terms of $\Delta\omega$ with any of the other variables since the integral over the energy coordinate will be dominated by the linear

term $\exp(-i\tau\Delta\omega)$. This is so because for spin-echo measurements to be sensible, the only case of interest is the situation where $\Delta\omega$ is very small and hence $S(\omega)$ is very narrow compared with the TAS energy resolution.

We can therefore write

$$P = \frac{1}{N}\int \exp\left(-\tfrac{1}{2}\widetilde{\mathbf{J}}^T\widetilde{\mathbf{L}}_\mathrm{I}\widetilde{\mathbf{J}}\right)\mathrm{d}\widetilde{J}_n \times \int S(\omega)\exp(-i\tau\Delta\omega)\,\mathrm{d}\Delta\omega + \text{c.c.} \qquad (62)$$

where $\widetilde{\mathbf{J}} = (\Delta k_\mathrm{in}, y_1, y_2, z_1, z_2)$ and $\widetilde{\mathbf{L}}_\mathrm{I}$ is the (5×5) submatrix with respect to the $(\Delta k_\mathrm{in}, y_1, y_2, z_1, z_2)$ subspace.

Equation (62) manifests an important result, *i.e.* the polarization is the product of the Fourier transform of the scattering function $S(\omega)$ and a τ-dependent function F_I which accounts for resolution, where

$$F_\mathrm{I}(\tau) = \frac{1}{N}\int \exp\left[-\tfrac{1}{2}\widetilde{\mathbf{J}}^T\widetilde{\mathbf{L}}_\mathrm{I}(\tau)\widetilde{\mathbf{J}}\right]\mathrm{d}\widetilde{J}_n + \text{c.c.} \qquad (63)$$

Since there is no convolution of the resolution function with the signal, this means that the result of a measurement can be corrected for resolution by dividing the data with $F_\mathrm{I}(\tau)$. Also, equation (63) follows immediately from equation (62) if we assume the excitation to have zero line width, *i.e.* $S(\omega) = \delta(\omega - \omega_0)$.

We will obtain the instrumental resolution as a function of spin-echo time by solving the integrals over the wavevector components Δk_in, y_1, y_2, z_1, z_2 in equation (63). In principle, this is possible by explicitly applying Gaussian integrals. This, however, yields little insight and it is more convenient to make use of the following general theorem (Miller, 1964; Zee, 2003):

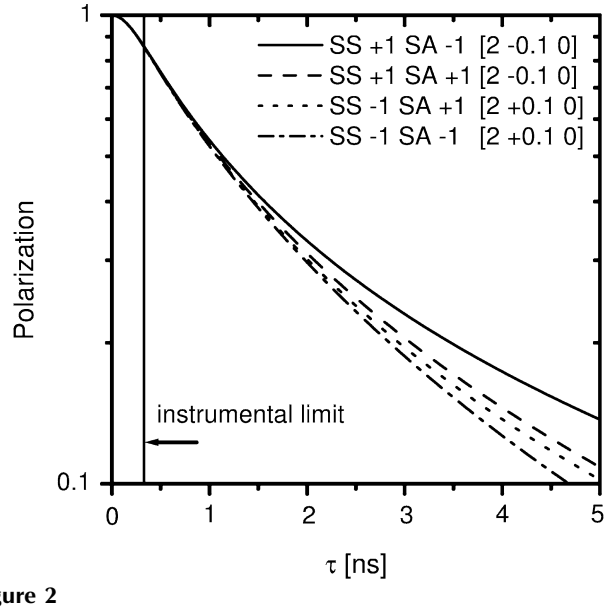

Figure 2
Calculated instrumental resolution, *i.e.* the polarization as a function of spin-echo time τ for the $[2 \pm 0.1\ 0]$ TA phonon. The phonon is assumed to have zero line width. The spectrometer configurations and the phonon coordinates in r.l.u. are given in the inset. The scattering sense at the monochromator is always $S_\mathrm{M} = -1$. Note that the spin-echo time in current NRSE apparatus for this specific phonon is limited to 330 ps, as indicated by the vertical line. Note the logarithmic scale in polarization.

$$\int_{-\infty}^{\infty} \exp\left(-\tfrac{1}{2}\mathbf{Y}^T\mathbf{M}\mathbf{Y}\right)\mathrm{d}^n Y_n = \frac{(2\pi)^{n/2}}{(\det\mathbf{M})^{1/2}}, \qquad (64)$$

where $\mathbf{Y}$ is an n-dimensional column vector and $\mathbf{M}$ is a positive-definite symmetric $(n \times n)$ matrix. In more formal detail, we are allowed to apply this integral theorem for quadratic forms since the Hermitian quantity $(\widetilde{\mathbf{L}}_\mathrm{I} + \widetilde{\mathbf{L}}_\mathrm{I}^*)$ is positive definite. Finally, we can write

$$F_\mathrm{I}(\tau) = \left|\left[\frac{\det\widetilde{\mathbf{L}}_\mathrm{I}(\tau = 0)}{\det\widetilde{\mathbf{L}}_\mathrm{I}(\tau)}\right]^{1/2}\right|. \qquad (65)$$

We will call F_I the instrumental resolution function since the depolarization depends solely on instrumental parameters. The normalization is chosen such that $F_\mathrm{I} = 1$ if $\tau = 0$.

2.6. Discussion

We have numerically evaluated the expression given in equation (65) for a typical set of TAS parameters and the transverse acoustic (TA) [2 0.1 0] phonon in Pb.[1] A spin-echo experiment investigating anharmonic phonon line widths in Pb has been performed recently with the NRSE instrument at the Hahn-Meitner-Institute, Berlin (Habicht *et al.*, 2003*a*). The [0 0.1 0] TA phonon has an energy of $\hbar\omega_0 = 0.88$ meV and a slope of the dispersion $|\hbar\nabla_q\omega_0(\mathbf{q}_0)| = 6.9$ meV Å at $T = 290$ K. In the calculation an incident wavenumber $k_\mathrm{I} = 1.7$ Å^{-1} has been assumed, which corresponds to the case of a cold-neutron TAS. For numerical values of TAS-related parameters see Appendix *A*. Note that a 'bootstrap' NRSE operated with a maximum RF frequency $\nu_\mathrm{max} = 800$ kHz gives $\tau_\mathrm{max} = 330$ ps. In Fig. 2, we show the instrumental resolution calculated for different spectrometer configurations for phonon creation, *i.e.* $\hbar\omega > 0$. The scattering senses are defined to be positive for scattering to the left. Note that for *e.g.* [2 +0.1 0], it is experimentally impossible to satisfy the spin-echo conditions in the ($S_\mathrm{M} = -1$, $S_\mathrm{S} = +1$, $S_\mathrm{A} = \pm 1$) configuration, since tilt angles >50° would be required. Depending on the spectrometer configuration, the resolution function differs only slightly, which is explained by the small differences in the TAS transmission function upon a change of spectrometer configuration. We note that significant differences between spectrometer configurations might appear in the case of thermal TAS instruments, where the resolution ellipsoid is much more anisotropic and inclined relative to the dispersion.

In conclusion, the depolarization due to the instrument can play a role within the experimentally accessible range of spin-echo times, since in the example the polarization $P(\tau_\mathrm{max}) = 0.85$. In the experiment investigating phonon line widths in Pb, τ was always less than 100 ps. Since $P(100\ \mathrm{ps}) = 0.98$, the instrumental resolution is negligible.

[1] The program code for computational calculations can be obtained from the correspondence author upon request.

3. Mosaic sample

As Pynn (1978) pointed out 'for transverse branches ... a further limit to resolution will be introduced by the crystal mosaic of the sample ...' Quantitatively, this is obvious from Fig. 3: the dispersion surface will have different orientations in space for different mosaic grains of the sample. Hence this effect gives rise to a smearing of the dispersion surface and therefore appears as a broadening in energy, which is different from any intrinsic line width of the excitations.

Let us reconsider equations (10) and (12). Taking mosaic into account we have

$$\mathbf{q} - \mathbf{q}_0 = \Delta\mathbf{k}_\mathrm{i} - \Delta\mathbf{k}_\mathrm{f} - \mathbf{G} + \mathbf{G}_0 \tag{66}$$

and

$$\Delta\mathbf{G} = \mathbf{G} - \mathbf{G}_0, \tag{67}$$

where $\mathbf{G}$ is a reciprocal-lattice vector which is tilted with respect to $\mathbf{G}_0$ by angles $\Delta\eta$ and $\Delta\nu$ in the scattering plane and vertically. This is equivalent to the treatment of sample mosaic given by Werner & Pynn (1971) in the case of the TAS resolution function.

The energy variation in equation (10) will now have an additional term proportional to $\nabla_q\omega_0(\mathbf{q}_0)\cdot\Delta\mathbf{G}$ and reads

$$\Delta\omega' = \Delta\omega + \nabla_q\omega_0(\mathbf{q}_0)\cdot\Delta\mathbf{G}. \tag{68}$$

We expand the variation in the reciprocal-lattice vector to second order in $\Delta\eta$, $\Delta\nu$:

$$\Delta\mathbf{G} = |\mathbf{G}_0|\begin{pmatrix} -\Delta\eta^2/2 - \Delta\nu^2/2 \\ \Delta\eta - \Delta\nu^2/2 \\ \Delta\nu \end{pmatrix}. \tag{69}$$

We will next investigate how the sample mosaicity affects the spin-echo amplitude for two extreme phonon examples: a transverse phonon and a longitudinal phonon.

3.1. Transverse phonon

Since the scattering function $S(\mathbf{Q},\omega)$ is proportional to $(\mathbf{Q}\cdot\mathbf{e})^2$, where $\mathbf{e}$ is the phonon polarization vector, for a transverse polarized phonon the direction of $\mathbf{q}_0$ will be best chosen perpendicular to $\mathbf{G}_0$. Hence for a transverse polarized phonon $\nabla_q\omega_0(\mathbf{q}_0)$ will be perpendicular to $\mathbf{G}_0$ and therefore

$$\nabla_q\omega_0(\mathbf{q}_0)\cdot\Delta\mathbf{G} = |\nabla_q\omega_0(\mathbf{q}_0)||\mathbf{G}_0|\left(\Delta\eta - \frac{\Delta\nu^2}{2}\right). \tag{70}$$

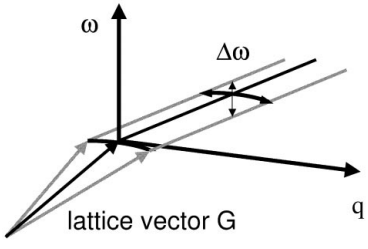

Figure 3
Effect of the mosaic spread on the width of the dispersion surface. The angular variation in the lattice vector $\mathbf{G}$ will broaden the dispersion in energy.

A more extended treatment includes all second-order terms and is given in §4. However, we see that the leading term will be of first order in $\Delta\eta$. Assuming a Gaussian mosaic distribution, the polarization $P(\tau)$ will be multiplied by an integral

$$\int \exp\left[-\tfrac{1}{2}\left(\frac{\Delta\eta}{\eta_\mathrm{S}}\right)^2 - i\tau|\nabla_q\omega_0(\mathbf{q}_0)||\mathbf{G}_0|(\Delta\eta)\right]\mathrm{d}\Delta\eta, \tag{71}$$

which has the solution

$$(2\pi\eta_\mathrm{S})^{1/2}\exp\left[-\tfrac{1}{2}\tau^2|\nabla_q\omega_0(\mathbf{q}_0)|^2|\mathbf{G}_0|^2\eta_\mathrm{S}^2\right], \tag{72}$$

i.e. a Gaussian with 1σ standard deviation $[|\nabla_q\omega_0(\mathbf{q}_0)||\mathbf{G}_0|\eta_\mathrm{S}]^{-2}$. For a dispersionless mode, sample mosaicity will not contribute to depolarization [$|\nabla_q\omega_0(\mathbf{q}_0)| = 0$]; however, polarization will decrease rapidly for a dispersive mode.

For the [2 0.1 0] TA example phonon in Pb, the polarization will be less than 10% beyond $\tau > 50$ ps if we assume a mosaic $\eta_\mathrm{S} = 5'$. Clearly this dominates over second-order effects considered so far.

In order to verify equation (71) we have measured the phase shift as a function of the angular sample orientation using a MnF_2 single crystal with very low mosaic spread. The angle of the sample with respect to the incident wavevector $\mathbf{k}_\mathrm{I}$ was varied at the [1 0 0.05] magnon which has an energy $\hbar\omega_0(\mathbf{q}_0) = 1.4$ meV and a dispersion with slope $|\hbar\nabla_q\omega_0(\mathbf{q}_0)| = 7.11$ meV Å at $T = 30$ K. The (1 0 0) reciprocal-lattice vector has value $G_0 = 1.29$ Å^{-1}. From these parameters we calculated tilt angles $\theta_1 = -14.4^\circ$ and $\theta_2 = 3.87^\circ$ and a frequency ratio of $\nu_1/\nu_2 = 1.185$. The measurement was performed at $k_\mathrm{I} = 2.0$ Å^{-1} at an effective frequency $\nu_2^\mathrm{eff} = 400$ kHz, which corresponds to $\tau = 23.5$ ps. The phase shift was experimentally determined by scanning a full period of the inelastic spin-echo signal at each

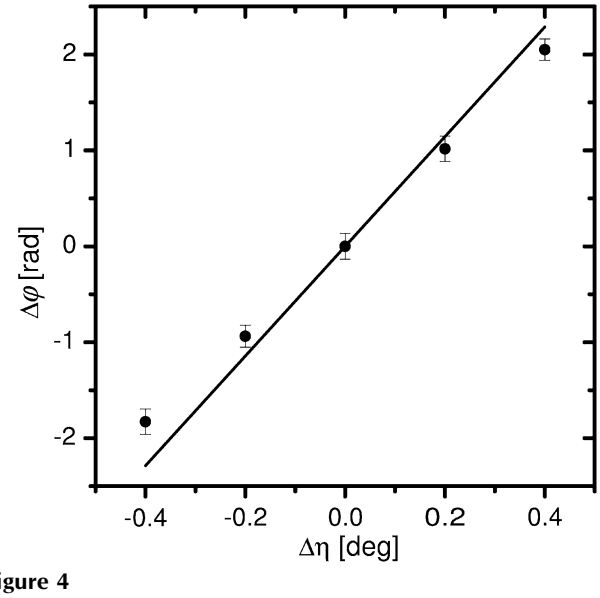

Figure 4
The phase shift of the inelastic signal as a function of the angular sample orientation $\Delta\eta$ measured at the [1 0 0.05] magnon in MnF_2. Symbols are experimental data. The line represents the phase shift as calculated from equation (73).

angular orientation of the sample. The theoretical phase shift is calculated from equation (71) as

$$\Delta\varphi = -\tau|\nabla_q\omega_0(\mathbf{q}_0)||\mathbf{G}_0|\Delta\eta. \quad (73)$$

The result of the measurement is shown in Fig. 4. Theory and experiment are in fair agreement showing the reasonableness of our assumptions.

3.2. Longitudinal phonon

Considering a longitudinal phonon, the direction of $\mathbf{q}_0$ will be best chosen parallel to $\mathbf{G}_0$ and

$$\nabla_q\omega_0(\mathbf{q}_0)\cdot\Delta\mathbf{G} = |\nabla_q\omega_0(\mathbf{q}_0)||\mathbf{G}_0|\left(-\frac{\Delta\eta^2}{2}-\frac{\Delta\nu^2}{2}\right). \quad (74)$$

Hence sample mosaic will only contribute in second order. A proper discussion will require a more extended framework which we will provide in the next section.

4. Effect of general lattice imperfections in NSE lifetime measurements

In this section we will follow the effect of lattice imperfections, namely horizontal and vertical mosaicity, as well as a distribution of d spacings, all assumed to be Gaussian, up to second order. We will outline the modifications to obtain extended expressions for the matrix $\mathbf{L}_\mathrm{I}$. We will then discuss the two extreme cases where the gradient of the dispersion surface is either perpendicular or parallel to the reciprocal-lattice vector $\mathbf{G}_0$.

The probability of a neutron hitting a mosaic block with a specific $\mathbf{G}$ can be formulated as

$$\exp\left[-\tfrac{1}{2}\left(\frac{\Delta\eta^2}{\eta_\mathrm{S}^2}+\frac{\Delta\nu^2}{\nu_\mathrm{S}^2}+\frac{\Delta G^2}{\Upsilon^2}\right)\right]. \quad (75)$$

Here $\Delta\eta$ is the tilt angle in the scattering plane with respect to $\mathbf{G}_0$, $\Delta\nu$ is the tilt angle out of the scattering plane and ΔG includes a spread in d spacings. η_S, ν_S and Υ are the 1σ standard deviations for Gaussian horizontal and vertical mosaic, and Gaussian distribution of lattice vectors, respectively.

We write small variations in the reciprocal-lattice vector expanded up to second order as

$$\Delta\mathbf{G} = \begin{bmatrix} \Delta G - \frac{1}{2}G_0(\Delta\eta^2-\Delta\nu^2) \\ (G_0+\Delta G)\Delta\eta - \frac{1}{2}G_0\Delta\nu^2 \\ (G_0+\Delta G)\Delta\nu \end{bmatrix}, \quad (76)$$

where the x component of this vector is parallel to $\mathbf{G}$.

Since the energy variation $\Delta\omega$ has an additional term due to sample imperfections [see equation (68)] we introduce a new column vector $\mathbf{J}_\mathrm{M} = (\Delta\omega, \Delta k_\mathrm{in}, y_1, y_2, z_1, z_2, \Delta G, \Delta\eta, \Delta\nu)$. The new vector $\mathbf{J}_\mathrm{M}$ includes the new variables and is given by the linear transform of the vector $\mathbf{J}$

$$\mathbf{J}_\mathrm{M} = \mathbf{I}\mathbf{J}, \quad (77)$$

where the non-zero elements of the (6×9) transformation matrix $\mathbf{I}$ are given by

$$I_{11} = I_{22} = I_{33} = I_{44} = I_{55} = I_{66} = 1, \quad (78)$$

$$I_{17} = C_x, \quad I_{18} = C_yG_0, \quad I_{19} = C_zG_0. \quad (79)$$

Here C_x is the component of the group velocity $\mathbf{C} = \nabla_q\omega_0(\mathbf{q}_0)$ along the reciprocal-lattice vector $\mathbf{G}_0$, C_y is the component of $\mathbf{C}$ right-handed perpendicular to $\mathbf{G}_0$ in the scattering plane, and C_z is the component of $\mathbf{C}$ perpendicular to $\mathbf{G}_0$ out of the scattering plane.

The new matrix which includes sample imperfections is then given by

$$\mathbf{L}_\mathrm{M} = \mathbf{I}^T\mathbf{L}_\mathrm{I}\mathbf{I} + \mathbf{N} + \mathbf{W} \quad (80)$$

where the (9×9) matrix $\mathbf{N}$ has non-zero elements

$$N_{77} = \frac{1}{\Upsilon_\mathrm{S}^2}, \quad N_{88} = \frac{1}{\eta_\mathrm{S}^2}, \quad N_{99} = \frac{1}{\nu_\mathrm{S}^2}, \quad (81)$$

and $\mathbf{W}$ accounts for the quadratic terms in ΔG, $\Delta\eta$ and $\Delta\nu$, which arise from the linear term $-i\tau\Delta\omega'$ in the exponent of equation (60). The symmetric (9×9) matrix $\mathbf{W}$ has non-zero elements

$$W_{78} = W_{87} = -i\tau C_y, \quad W_{79} = W_{97} = -i\tau C_z, \quad (82)$$

$$W_{88} = -i\tau C_xG_0, \quad W_{99} = -i\tau(C_x - C_y)G_0. \quad (83)$$

As emphasized in the preceding section, we have also linear terms in ΔG, $\Delta\eta$ and $\Delta\nu$ which we write as $\mathbf{T}_\mathrm{M}^T\mathbf{J}_\mathrm{M}$ where the column vector $\mathbf{T}_\mathrm{M} = i\tau(0, 0, 0, 0, 0, 0, C_x, C_yG_0, C_zG_0)$.

We can now write

$$2\langle\sigma_x\rangle = \frac{1}{N}\int S(\mathbf{Q},\omega)\exp(-i\tau\Delta\omega)\exp\left(\mathbf{T}_\mathrm{M}^T\mathbf{J}_\mathrm{M}\right) \times \exp\left(-\tfrac{1}{2}\mathbf{J}_\mathrm{M}^T\mathbf{L}_\mathrm{M}\mathbf{J}_\mathrm{M}\right)\mathrm{d}J_{\mathrm{M},n} + \mathrm{c.c.} \quad (84)$$

We assume again that $S(\mathbf{Q},\omega) = S(\omega)$, *i.e.* the scattering function is independent of $\mathbf{Q}$, and can separate the resolution by neglecting the terms in $\Delta\omega$ higher than first order. We thus write

$$F_\mathrm{M} = \frac{1}{N}\int \exp\left(\widetilde{\mathbf{T}}_\mathrm{M}^T\widetilde{\mathbf{J}}_\mathrm{M}\right)\exp\left(-\tfrac{1}{2}\widetilde{\mathbf{J}}_\mathrm{M}^T\widetilde{\mathbf{L}}_\mathrm{M}\widetilde{\mathbf{J}}_\mathrm{M}\right)\mathrm{d}\widetilde{J}_{\mathrm{M},n} + \mathrm{c.c.} \quad (85)$$

where $\widetilde{\mathbf{J}}_\mathrm{M} = (\Delta k_\mathrm{in}, y_1, y_2, z_1, z_2, \Delta G, \Delta\eta, \Delta\nu)$, $\widetilde{\mathbf{T}}_\mathrm{M} = i\tau(0, 0, 0, 0, 0, C_x, C_yG_0, C_zG_0)$ and $\widetilde{\mathbf{L}}_\mathrm{M}$ is the (8×8) submatrix with respect to the $(\Delta k_\mathrm{in}, y_1, y_2, z_1, z_2\Delta G, \Delta\eta, \Delta\nu)$ subspace. We make use of the general theorem (Miller, 1964)

$$\int_{-\infty}^{\infty}\exp\left(\mathbf{T}^T\mathbf{Y}\right)\exp\left(-\tfrac{1}{2}\mathbf{Y}^T\mathbf{M}\mathbf{Y}\right)\mathrm{d}^nY_n = \frac{(2\pi)^{n/2}}{(\det\mathbf{M})^{1/2}}\exp\left(\tfrac{1}{2}\mathbf{T}^T\mathbf{M}^{-1}\mathbf{T}\right). \quad (86)$$

The generalized resolution function now includes Gaussian-approximated sample imperfections and can be expressed as

$$F_\mathrm{M} = \left|\left[\frac{\det\widetilde{\mathbf{L}}_\mathrm{M}(\tau=0)}{\det\widetilde{\mathbf{L}}_\mathrm{M}(\tau)}\right]^{1/2}\exp\left(\tfrac{1}{2}\widetilde{\mathbf{T}}^T\widetilde{\mathbf{L}}_\mathrm{M}^{-1}\widetilde{\mathbf{T}}\right)\right|. \quad (87)$$

We will now give examples for the two extreme cases where the gradient of the dispersion surface is either perpendicular or parallel to the reciprocal-lattice vector $\mathbf{G}_0$.

4.1. Transverse phonon

The polarization as a function of spin-echo time for the [2 +0.1 0] TA Pb phonon assuming zero line width is shown in Fig. 5. Mosaicity is a parameter. The curves are calculated from equation (87).

The dominating term which causes the polarization to decay is

$$\left|\exp\left(\tfrac{1}{2}\widetilde{\mathbf{T}}^T\widetilde{\mathbf{L}}_{\mathrm{M}}^{-1}\widetilde{\mathbf{T}}\right)\right| = \exp\left(-\tfrac{1}{2}\tau^2 C_y^2 G_0^2 \eta_{\mathrm{S}}^2\right), \tag{88}$$

as derived in equation (72). This exponential decay with quadratic τ dependence is a consequence of the fact that mosaicity appears in the spin-echo phase in first order.

4.2. Longitudinal phonon

Considering a longitudinal excitation it is ΔG which appears in first order in the spin-echo phase.

The dominating term is then

$$\left|\exp\left(\tfrac{1}{2}\widetilde{\mathbf{T}}^T\widetilde{\mathbf{L}}_{\mathrm{M}}^{-1}\widetilde{\mathbf{T}}\right)\right| = \exp\left(-\tfrac{1}{2}\tau^2 C_x^2 \Upsilon^2\right). \tag{89}$$

Typical deviations in lattice spread are of the order of 10^{-4} for standard crystals. Note that Υ depends linearly on the magnitude of the reciprocal-lattice vector, *i.e.* $\Upsilon = 10^{-4} G_0$. The resulting polarization as a function of spin-echo time is given in Fig. 6 for the [1.9 0 0] LA phonon in Pb, which has an energy of 1.65 meV and a gradient C_y = 13 meV Å at T = 290 K. The example was calculated for k_{I} = 1.52 Å^{-1}. This gives a scattering angle at the sample $2\theta_{\mathrm{S}} = 122^\circ$ and tilt angles $\theta_1 = 17.3^\circ$, $\theta_2 = -49.5^\circ$ without reversal of the relative field directions in the first and second precession region, *i.e.* $B_1 || B_2$. We have calculated the polarization from the total resolution function, *i.e.* from equation (87). We see that instrumental resolution and sample-related resolution are comparable if $\Upsilon \simeq 10^{-5} G_0$. To give an idea how sample mosaicity affects the resolution in measurements of longitudinal excitations, we have also included the resolution function for $\Upsilon = 0$, but $\Delta\eta = \Delta\nu = 60'$. The sample can have rather large mosaic spreads before these play an important role in resolution.

5. Curvature of the dispersion surface

In addition to instrumental resolution and lattice imperfections, there is another effect to be considered in lifetime measurements of elementary excitations distinct from intrinsic line-width broadening. If the dispersion surface is significantly curved within the resolution ellipsoid of the background TAS, this leads to a decrease in polarization depending on the spin-echo time.

Let us consider a perfect sample without any lattice distortions, such as mosaicity or variation of d spacings. The curvature of the dispersion surface is included by the second-order derivatives in the expansion of the dispersion relation. Equation (26) will then have an additive term

$$-\tfrac{1}{2}\Delta\mathbf{q}^T\mathbf{H}\Delta\mathbf{q}. \tag{90}$$

Here $\mathbf{H}$ is the symmetric (3 × 3) Hessian which is defined as

$$\mathbf{H} = \mathbf{R}^T\mathbf{H}'\mathbf{R}, \tag{91}$$

with

$$H'_{ij} = \frac{\partial^2}{\partial q_i \partial q_j}\omega(q)\bigg|_{q=q_0}. \tag{92}$$

$\mathbf{H}'$ is expressed in coordinates of the reciprocal lattice. The matrix $\mathbf{R}$ transforms $\mathbf{H}'$ such that $\mathbf{H}$ is expressed in the coordinate system of $\mathbf{Q}$, *i.e.* $\mathbf{i}_0$, $\mathbf{j}_0$, $\mathbf{l}_0$ (Fig. 1). For simplicity we

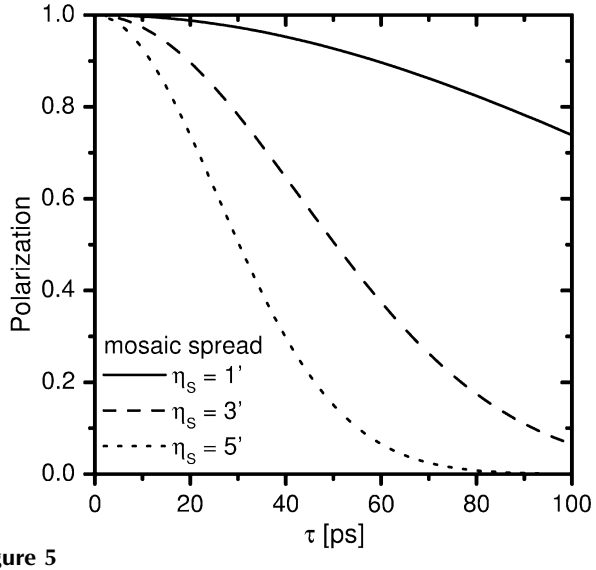

Figure 5
Effect of mosaic spread on the polarization of the inelastic signal. The curves are calculated for the [2 +0.1 0] TA phonon in Pb. Note that the mosaic spread η_{S} is the 1σ standard deviation.

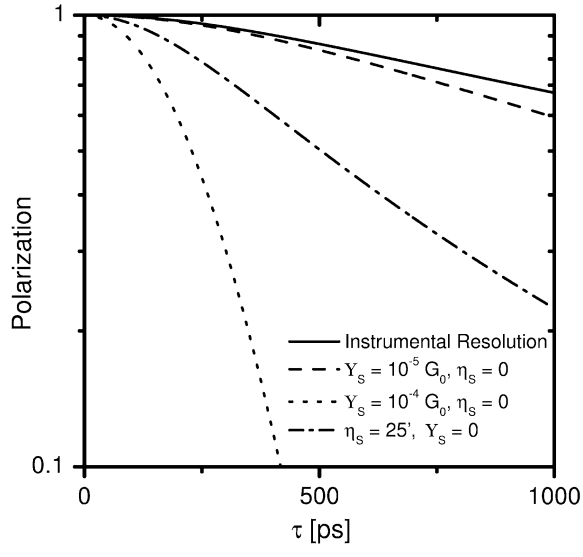

Figure 6
The resolution function for a sample with lattice imperfections. The curves are calculated for the [1.9 0 0] LA phonon in Pb. Note the logarithmic scale in polarization.

restrict ourselves to a tetragonal crystal with the (a^*, b^*) plane being the scattering plane and $\mathbf{R}$ being a simple rotation matrix

$$\mathbf{R} = \begin{pmatrix} f & d & 0 \\ -d & f & 0 \\ 0 & 0 & 1 \end{pmatrix} \tag{93}$$

with

$$d = -\sin\vartheta, \quad f = \cos\vartheta, \tag{94}$$

$$a = \sin\Phi, \quad b = \cos\Phi, \tag{95}$$

$$A = \sin\Xi, \quad B = -\cos\Xi, \tag{96}$$

where ϑ is the angle between $\mathbf{Q}$ and $\mathbf{q}$, Φ is the angle between $\mathbf{k}_\mathrm{I}$ and $-\mathbf{Q}$, and Ξ is the angle between $\mathbf{Q}$ and $\mathbf{k}_\mathrm{F}$. Also, $\Delta\mathbf{q}$ can be expressed in the coordinate system of $\mathbf{Q}$ as

$$\Delta\mathbf{q} = \mathbf{k}_\mathrm{i} - \mathbf{k}_\mathrm{f} = \begin{pmatrix} bx_1 + ay_1 - Bx_2 - Ay_2 \\ -ax_1 + by_1 + Ax_2 - By_2 \\ z_1 - z_2 \end{pmatrix}. \tag{97}$$

The modified matrix which includes the effect of a curved dispersion surface is given by

$$\mathbf{L}_\mathrm{C} = \mathbf{L}_\mathrm{I} + i\tau\mathbf{I}_\mathrm{C}^T\mathbf{\Theta}^T\mathbf{H}\mathbf{\Theta}\mathbf{I}_\mathrm{C}, \tag{98}$$

where the purpose of the transformation matrix $(\mathbf{\Theta}\mathbf{I}_\mathrm{C})$ is to transform the Hessian $\mathbf{H}$ into the appropriate coordinate space of $\mathbf{L}_\mathrm{I}$. The matrix $\mathbf{\Theta}$ describes the transformation

$$\Delta\mathbf{q} = \mathbf{\Theta}\mathbf{Y}, \tag{99}$$

where the column vector $\mathbf{Y} = (x_1, y_1, z_1, x_2, y_2, z_2)$ and $\mathbf{\Theta}$ is given by

$$\mathbf{\Theta} = \begin{pmatrix} b & a & 0 & -B & -A & 0 \\ -a & b & 0 & A & -B & 0 \\ 0 & 0 & 1 & 0 & 0 & -1 \end{pmatrix}. \tag{100}$$

$\mathbf{I}_\mathrm{C}$ relates $\mathbf{Y}$ and $\mathbf{J}$ with the linear transformation $\mathbf{Y} = \mathbf{I}_\mathrm{C}\mathbf{J}$. The non-zero elements of the (6×6) matrix $\mathbf{I}_\mathrm{C}$ are given by

$$I_{\mathrm{C}12} = \frac{1}{\cos\theta_1}, \quad I_{\mathrm{C}13} = -\tan\theta_1, \tag{101}$$

$$I_{\mathrm{C}41} = -\frac{1}{N_\mathrm{F}\cos\theta_2}, \quad I_{\mathrm{C}42} = \frac{N_\mathrm{I}}{N_\mathrm{F}\cos\theta_2}, \tag{102}$$

$$I_{\mathrm{C}44} = -\tan\theta_2, \tag{103}$$

$$I_{\mathrm{C}23} = I_{\mathrm{C}35} = I_{\mathrm{C}54} = I_{\mathrm{C}66} = 1. \tag{104}$$

Finally, the resolution function which includes instrumental effects and depolarization due to curvature of the dispersion surface is given by

$$F_\mathrm{C} = \left| \left[\frac{\det\widetilde{\mathbf{L}}_\mathrm{C}(\tau = 0)}{\det\widetilde{\mathbf{L}}_\mathrm{C}(\tau)} \right]^{1/2} \right|, \tag{105}$$

where $\widetilde{\mathbf{L}}_\mathrm{C}$ is the (5×5) submatrix with respect to the $(\Delta k_\mathrm{in}, y_1, y_2, z_1, z_2)$ subspace.

If curvature of the dispersion surface is to be considered in an imperfect sample, we account for all sample- and instrument-related resolution effects if in equation (80) $\mathbf{L}_\mathrm{I}$ is replaced by $\mathbf{L}_\mathrm{C}$ and equation (87) gives the total resolution function.

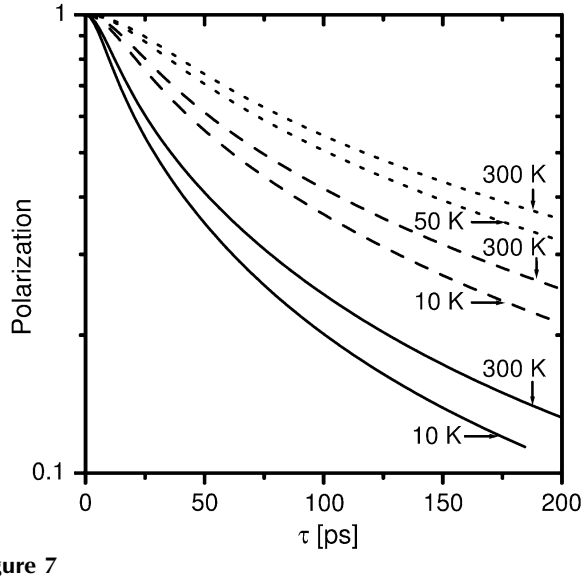

Figure 7
Depolarization due to curvature of the dispersion surface for the [2 ξ 0] TA phonon in Pb. ξ = 0.05 r.l.u. (solid), ξ = 0.10 r.l.u. (dashed), ξ = 0.15 r.l.u. (dotted). The intrinsic phonon line width has been assumed to vanish, *i.e.* Γ = 0.

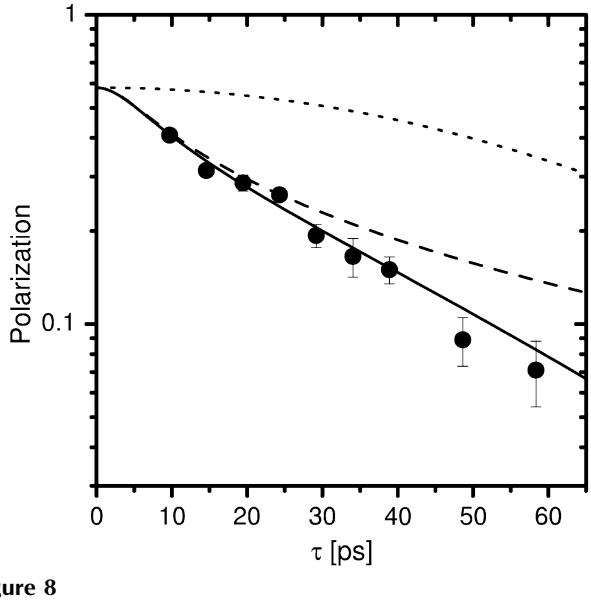

Figure 8
The [0.025 0.025 0] TA phonon in Pb at T = 50 K. Depolarization due to mosaic spread (dotted) with $\eta_\mathrm{S} = 1.8'$, curvature of the dispersion surface (dashed) and the combined effect of both (solid line). Solid circles: experimental data of an NRSE line-width measurement.

5.1. Discussion and experimental verification

As an example we consider again transverse acoustic phonons in Pb. For determination of the curvature parameters we approximate the dispersion by the expression

$$\hbar\omega_0(\mathbf{q}) = E_h\Big[\sin^2\Big(\frac{\pi}{2}q_h\Big) + \sin^2\Big(\frac{\pi}{2}q_k\Big) + \sin^2\Big(\frac{\pi}{2}q_l\Big)\Big]^{1/2}, \tag{106}$$

which is a reasonable approximation of the dispersion in the small-q limit. Here E_h is the phonon energy at the Brillouin zone boundary and q_h, q_k, q_l are the components of the phonon wavevector in r.l.u. along $\mathbf{a}^*$, $\mathbf{b}^*$, $\mathbf{c}^*$. The elements of the Hessian $\mathbf{H}$ are then given by the second-order derivatives of equation (106). In Fig. 7 we show the τ dependence of the polarization as calculated from equation (105). We see that the resolution function significantly varies with the phonon wavevector q. Hence, in general it is not justified to assume a resolution function which is independent of q. The variation with temperature is less significant.

In Fig. 8 we compare the calculated τ dependence of the polarization with experimental data which were collected in the study of anharmonic line widths in Pb. The calculated resolution curves have been normalized with a τ-independent constant: the experimentally determined polarization from [2 0 0] Bragg scattering since the experimental calibration with the elastic signal shows very little variation with τ. Although in the inelastic signal there is significant depolarization, the decay of the polarization can be explained entirely by the mosaicity of the sample and the curvature of the dispersion. Within statistics the intrinsic phonon line width is consistent with zero.

We have shown that sample mosaicity and curvature of the dispersion surface can lead to a significant depolarization in a high-resolution experiment combining the N(R)SE and TAS neutron scattering techniques. If this is the case, the measured polarization should be corrected for resolution by dividing the experimental polarization with the resolution function. Since the resolution function is inaccessible experimentally, in most cases one has to rely on the calculated resolution. In Fig. 9 we present line widths as obtained from raw data and corrected data.

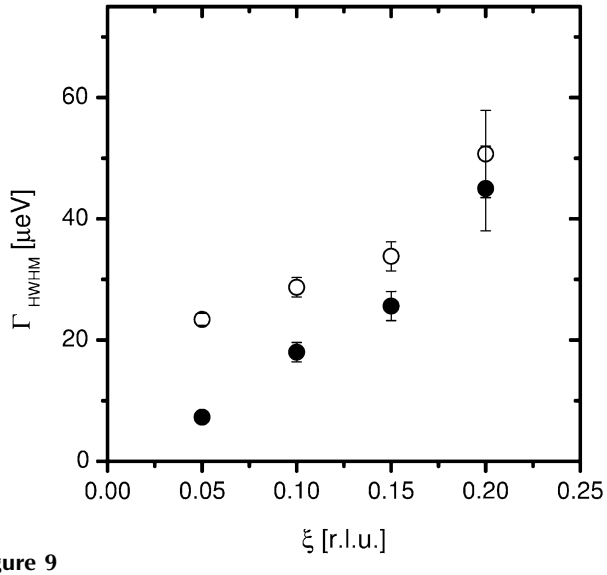

Figure 9
Phonon line widths of the [ξ 0 0] TA mode in Pb. Open symbols: line widths obtained from a fit to raw data. Solid symbols: line widths obtained from a fit to data corrected for curvature of the dispersion surface and mosaic spread.

6. Conclusions

The theory of inelastic neutron spin-echo spectroscopy has been extended to second order. Thus resolution effects are taken into account. The polarization as a function of spin-echo time is obtained for the general case of a dispersive excitation. Mosaicity is of particular importance in the determination of lifetimes of dispersive transverse excitation modes. The experiment confirms the depolarization due to sample mosaic. We have included curvature of the dispersion surface in our considerations of the resolution and have shown curvature to be a significant source of depolarization under experimental conditions. Our approach offers the opportunity to calculate resolution effects with N(R)SE-TAS instrumentation and to use the results for detailed planning of N(R)SE-TAS experiments.

Instrumental resolution can be separated from the signal since the resolution and the signal factorize. Hence the approach can be used for data correction of experimental results in N(R)SE-TAS experiments. This is of particular importance since in general an experimental calibration of the inelastic signal is not possible and the only clue to absolute line-width determinations is the calculated resolution.

APPENDIX *A*
Definition of TAS-related quantities

The quantities b_{0-5} and a_{11}^2, a_{12}^2 as used in equation (46) are defined to be

$$b_0 = a_1a_2 + a_7a_8, \tag{107}$$

$$b_1 = a_2^2 + a_3^2 + a_8^2, \tag{108}$$

$$b_2 = a_4^2 + a_6^2 + a_{10}^2, \tag{109}$$

$$b_3 = a_5^2 + a_9^2, \tag{110}$$

$$b_4 = a_5a_6 + a_9a_{10}, \tag{111}$$

$$b_5 = a_1^2 + a_7^2, \tag{112}$$

and

$$a_1 = \frac{\tan\theta_M}{\eta_M k_I}, \quad a_2 = \frac{1}{\eta_M k_I}, \quad a_3 = \frac{1}{\alpha_1 k_I}, \tag{113}$$

$$a_4 = \frac{1}{\alpha_2 k_F}, \quad a_5 = \frac{\tan\theta_A}{\eta_A k_F}, \quad a_6 = -\frac{1}{\eta_A k_F}, \tag{114}$$

$$a_7 = \frac{2\tan\theta_M}{\alpha_0 k_I}, \quad a_8 = \frac{1}{\alpha_0 k_I}, \quad a_6 = \frac{2\tan\theta_A}{\alpha_3 k_F}, \tag{115}$$

$$a_{10} = -\frac{1}{\alpha_3 k_F}, \tag{116}$$

$$a_{11}^2 = \left(\frac{1}{4\eta_M'^2 \sin^2\theta_M + \beta_0^2} + \frac{1}{\beta_1^2}\right)\frac{1}{k_I^2}, \tag{117}$$

$$a_{12}^2 = \left(\frac{1}{4\eta_A'^2 \sin^2\theta_A + \beta_3^2} + \frac{1}{\beta_2^2}\right)\frac{1}{k_F^2}. \tag{118}$$

All quantities except a_{11}^2, a_{12}^2 are as defined by Cooper & Nathans (1967). The latter quantities are correctly defined according to Dorner (1972). The same notation as employed by Cooper & Nathans (1967) is used, *i.e.* γ_i and δ_i are defined to be the horizontal and vertical divergence angles with respect to the optimum directions, respectively, and $i = 0, 1, 2, 3$, refer to in-pile, monochromator-to-sample, sample-to-analyser, and analyser-to-detector regions, respectively. η_M, η_M' and η_A, η_A' are the horizontal and vertical monochromator and analyser mosaic angles (1σ standard deviation) where $\Delta\eta_M$, $\Delta\eta_A$ are the horizontal and $\Delta\eta_M'$, $\Delta\eta_A'$ are the vertical tilts of the reflecting crystallites. α_i, β_i are the characteristic horizontal and vertical collimator angles. k_I and k_F are the most probable incident and final wavevectors if the monochromator and analyser angles are set to θ_M, θ_A.

Except where differently stated, all numerical calculations presented here use values appropriate for the NRSE instrument combined with the TAS V2 at the Berlin Neutron Scattering Centre. θ_M, θ_A are calculated from the d spacings of the monochromator and analyser, which are $d_{M,A} = 3.355$ Å, corresponding to the 002 reflection of pyrolytic graphite.

$$\begin{array}{llll} \eta_M = 30', & \eta_M' = 30', & \eta_A = 30', & \eta_A' = 30', \\ \alpha_0 = 50', & \alpha_0 = 30', & \alpha_0 = 30', & \alpha_0 = 30', \\ \beta_0 = 50', & \beta_0 = 85', & \beta_0 = 110', & \beta_0 = 380'. \end{array} \tag{119}$$

Mosaicity and collimation parameters are given as FWHM. Except where differently stated, scattering senses at the monochromator, sample and analyser are chosen to be $S_M = -1$, $S_S = -1$and $S_A = +1$, where the positive sign refers to scattering to the left.

Valuable discussions with R. Pynn are gratefully acknowledged.

References

Cooper, M. & Nathans, R. (1967). *Acta Cryst.* **23**, 357–367.
Dorner, B. (1972). *Acta Cryst.* A**28**, 319–327.
Gähler, R., Habicht, K., Keller, T. & Golub, R. (1996). *Physica B*, **229**, 1–17.
Habicht, K., Gähler, R., Golub, R. & Keller, T. (2003*a*). *Neutron Spin Echo Spectroscopy*. Berlin: Springer.
Habicht, K., Golub, R., Keimer, B., Mezei, F. & Keller, T. (2003*b*). In preparation.
Keller, T., Gähler, R. & Golub, R. (2002). In *Scattering*, edited by R. Pike & P. Sabatier, pp. 1264–1286. New York: Academic Press.
Mezei, F. (1978). *Inelastic Neutron Scattering*. Vienna: IAEA.
Mezei, F. (1980). *Neutron Spin Echo*. Berlin: Springer.
Miller, K. (1964). *Multidimensional Gaussian Distributions*. New York: John Wiley.
Popovici, M. (1975). *Acta Cryst.* A**31**, 507–513.
Pynn, R. (1978). *J. Phys. E*, **11**, 1133–1140.
Stoica, A. (1975). *Acta Cryst.* A**31**, 189–192.
Werner, S. & Pynn, R. (1971). *J. Appl. Phys.* **4212**, 4736–4749.
Zee, A. (2003). *Quantum Field Theory in a Nutshell*. Princeton University Press.